

Coseismic and postseismic stress changes in a subducting plate: Possible stress interactions between large interplate thrust and intraplate normal-faulting earthquakes

Takeshi Mikumo

Instituto de Geofísica, Universidad Nacional Autónoma de México, México D.F., México

Yuji Yagi

Earthquake Research Institute, University of Tokyo, Tokyo, Japan

Shri Krishna Singh and Miguel A. Santoyo

Instituto de Geofísica, Universidad Nacional Autónoma de México, México D.F., México

Received 13 February 2001; revised 31 August 2001; accepted 12 September 2001; published 30 January 2002

[1] A large intraplate, normal-faulting earthquake ($M_w = 7.5$) occurred in 1999 in the subducting Cocos plate below the downdip edge of the ruptured thrust fault of the 1978 Oaxaca, Mexico, earthquake ($M_w = 7.8$). This situation is similar to the previous case of the 1997 normal-faulting event ($M_w = 7.1$) that occurred beneath the rupture area of the 1985 Michoacan, Mexico, earthquake ($M_w = 8.1$). We investigate the possibility of any stress interactions between the preceding 1978 thrust and the following 1999 normal-faulting earthquakes. For this purpose, we estimate the temporal change of the stress state in the subducting Cocos plate by calculating the slip distribution during the 1978 earthquake through teleseismic waveform inversion, the dynamic rupture process, and the resultant coseismic stress change, together with the postseismic stress variations due to plate convergence and the viscoelastic relaxation process. To do this, we calculate the coseismic and postseismic changes of all stress components in a three-dimensional space, incorporating the subducting slab, the overlying crust and uppermost mantle, and the asthenosphere. For the coseismic stress change we solve elastodynamic equations, incorporating the kinematic fault slip as an observational constraint under appropriate boundary conditions. To estimate postseismic stress accumulations due to plate convergence, a virtual backward slip is imposed to lock the main thrust zone. The effects of viscoelastic stress relaxations of the coseismic change and the back slip are also included. The maximum coseismic increase in the shear stress and the Coulomb failure stress below the downdip edge of the 1978 thrust fault is estimated to be in the range between 0.5 and 1.5 MPa, and the 1999 normal-faulting earthquake was found to take place in this zone of stress increase. The postseismic variations during the 21 years after the 1978 event modify the magnitude and patterns of the coseismic stress change to some extent but are not large enough to overcome the coseismic change. These results suggest that the coseismic stress increase due to the 1978 thrust earthquake may have enhanced the chance of occurrence of the 1999 normal-faulting event in the subducting plate. If this is the case, one of the possible mechanisms could be static fatigue of rock materials around preexisting weak planes involved in the subducting plate, and it is speculated that that one of these planes might have been reactivated and fractured because of stress corrosion cracking under the applied stress there for 21 years. **INDEX TERMS:** 7209 Seismology: Earthquake dynamics and mechanics, 7260 Seismology: Theory and modeling, 8123 Tectonophysics: Dynamics, seismotectonics, 8164 Tectonophysics: Stresses—crust and lithosphere; **KEYWORDS:** Thrust earthquakes, Normal-faulting earthquakes, Waveform inversion, Subducting plate, Stress interactions

1. Introduction

[2] In the south Pacific coastal region of Mexico, where the Cocos plate subducts beneath the North American plate, large thrust earthquakes with low dip angles and shallow depths occur with relatively short recurrence time intervals [e.g., Singh *et al.*, 1981; Chael and Stewart, 1982; Pardo and Suarez, 1995]. In addition, large intermediate-depth, normal-faulting earthquakes also take place in the subducting plate [Singh *et al.*, 1985; Pardo

and Suarez, 1995; Cocco *et al.*, 1997]. While in other circum-Pacific subduction zones this type of intraplate event often takes place near the trench or the outer rise, some far updip of the thrust plane [Kanamori, 1971; Abe, 1972a, 1972b, 1977; Eissler and Kanamori, 1982; Spence, 1986; Christensen and Lay, 1988; Lundgren and Okal, 1988; Lynnes and Lay, 1988; Kausel and Campos, 1992; Yoshida *et al.*, 1992], and some have been interpreted to be caused by tensile stress due to the gravitational pull, most of the large, lithospheric normal-faulting events in the Mexican subduction zone occur mainly farther downdip in the unbending or the subhorizontal portion of the subducted Cocos plate [Pardo and Suarez, 1995; Singh *et al.*, 2000a; J. R. Gonzalez-Ruiz *et al.*, unpublished manuscript, 1984].

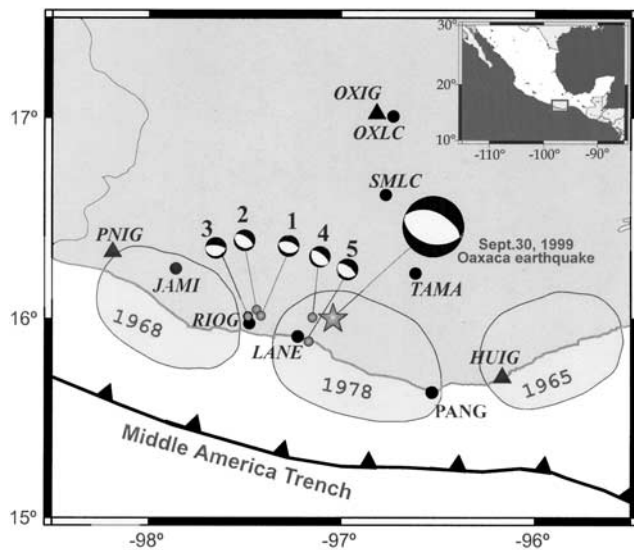


Figure 1. Location of the 30 September 1999 Oaxaca earthquake ($M_w = 7.5$) and its five aftershocks with magnitudes ranging between 4.0 and 4.6 (events 1–5) and the aftershock zones of the 1978 and two previous large thrust earthquakes in the Oaxaca region of the Mexican subduction zone. The fault plane solutions for the 1999 main shock and aftershocks are from the Harvard CMT solution and from local near-source stations, respectively (modified from Singh *et al.* [2000b]). Solid triangles (OXIG, PNIG, and HUIG) are broadband seismic stations; solid circles (OXLC, SMLC, JAMI, RIOG, LANE, TAMA, and PANG) show accelerometer stations.

[3] It is to be noted, however, that there are a few remarkable exceptions. In 1997 a large, nearly vertical, normal-faulting earthquake ($M_w = 7.1$) took place right below the extensively ruptured, thrust fault of the 1985 Michoacan earthquake ($M_w = 8.1$) [Mikumo *et al.*, 1999; M. A. Santoyo *et al.*, manuscript in preparation, 2001]. Another large, obliquely dipping, normal-faulting earthquake ($M_w = 7.5$) also occurred in 1999 just beneath the downdip edge of the thrust plane of the 1978 Oaxaca earthquake ($M_w = 7.8$), as shown in Figure 1 [Singh *et al.*, 2000b]. The 1931 Oaxaca, normal-faulting earthquake ($M_w = 7.8$) [Singh *et al.*, 1985] following the four large thrust events ($7.4 < M_s < 7.8$) of 1928 appears to have a location similar to that of the above two cases, although their epicentral locations may be more uncertain. The time interval between the two types of the above earthquakes is much shorter than the recurrence time of thrust events in this subduction zone.

[4] These observations lead us to expect that there might be some causal relationship or stress interactions between the preceding large thrust events and the following normal-faulting earthquakes. For the case of the 1985 Michoacan earthquake the dynamic rupture and coseismic stress change have been calculated [Mikumo *et al.*, 1999] from the distribution of kinematic slip over the fault plane with a dimension of 180 km \times 140 km dipping at 14°, which had been estimated from waveform inversion of local strong motion and teleseismic records [Mendoza and Hartzell, 1989]. These calculations reveal four high stress drop (stress decrease) zones with a maximum stress drop of 130 bars (13 MPa) and negative stress drop (stress increase) zones existing on the dipping fault. The maximum coseismic changes in the vertical shear stress and the Coulomb failure stress in the subducting slab reach the order of 0.4–0.8 MPa, \sim 30 km beneath the high stress drop zone on the fault plane. The rupture starting point and the major part of the 1997 vertical fault (M. A. Santoyo *et al.*, manuscript in preparation, 2001) are found to be located

within this zone of maximum stress increase [Mikumo *et al.*, 1999, 2000]. The above evidence suggests that the 1997 normal-faulting earthquake may have taken place under the effect of possible stress transfer from the 1985 thrust earthquake to the interior of the subducting Cocos plate.

[5] However, since the above calculations were only for coseismic stress change due to a large thrust event, it is undoubtedly necessary to estimate the postseismic stress change in the subducting plate to investigate the possibility of stress interactions in more detail. The goal of the present study is to investigate (1) the temporal change of the stress state not only in the subducting slab but in the overlying crust and uppermost mantle and in the lithosphere, through the kinematic and dynamic rupture process of thrust earthquakes and coseismic stress change, and (2) the postseismic changes due to plate convergence and viscoelastic relaxation process. In this study, we investigate the case of the large thrust Oaxaca earthquake in order to see if the coseismic and postseismic stress changes after the thrust event would enhance the chance of occurrence of the 1999 normal-faulting earthquake.

2. Rupture Processes of the 1978 and 1999 Oaxaca Earthquakes

[6] The 29 November 1978, thrust earthquake took place in the Oaxaca region of the Mexican subduction zone. The main shock was located at 15.77°N, 96.80°W [Ponce *et al.*, 1980; McNally and Minster, 1981] at a depth of 18 km [Stewart *et al.*, 1981]. Local seismic observations with portable field seismographs showed that the aftershocks were distributed over an area of \sim 80 km (in the E-W direction) \times 65 km (in the N-S direction) and that their hypocenters had increasing depths inland from the trench [Singh *et al.*, 1980], as shown in Figure 2. The fault plane solution has been obtained from *P* wave first motions at the World-Wide Standardized Seismograph Network (WWSSN) and Mexican stations, yielding two nodal planes ($\delta = 14^\circ$, $\phi = 270^\circ$ and $\delta = 79^\circ$, $\phi = 127^\circ$ [Stewart *et al.*, 1981]), and the northward dipping nodal plane at \sim 14° has been taken as the fault plane to be consistent with the depth distribution of aftershocks. The seismic moment estimated from WWSSN or Seismic Research Observatory (SRO) body wave data ranges between $1.6\text{--}1.9 \times 10^{27}$ dyn cm [Stewart *et al.*, 1981] and $\sim 3 \times 10^{27}$ dyn cm [Ward, 1980; Reichle *et al.*, 1980], and the estimates from WWSSN or International Deployment of Accelerometers (IDA) surface wave data are $2\text{--}3 \times 10^{27}$ dyn cm [Masters *et al.*, 1980] and 3.2×10^{27} dyn cm [Stewart *et al.*, 1981]. Comparison of the teleseismic *P* waveforms recorded at four WWSSN stations with the synthetic waveforms calculated from a simple point source model suggests that the source of this earthquake was very simple [Stewart *et al.*, 1981]. Following this suggestion, we assume, as a first step, simple slip distribution over a rectangular fault with a dimension of 85 km \times 65 km, fixing the seismic moment to 3.2×10^{27} dyn cm as estimated above; a possible distribution has elliptical-shaped slip amplitude as expected from a simple crack model, which is assumed to have a peak of 180 cm at the center of the fault and to decay along the length and width toward the fault edges. This gives an almost constant stress drop of \sim 13 bars except for stress increase near the peripheral fault zones. We will compare the results from this preliminary assumption with the final results from the slip distribution obtained from the waveform inversion described below.

[7] As a second step, we looked for more, long-period WWSSN records in order to estimate the actual slip distribution over the fault through waveform inversions. We were able to find their microfiche films, which are still well preserved at the seismogram library of Earthquake Research Institute, University of Tokyo, Japan. From these films, 27 horizontal and 8 vertical component records from 21 stations have been retrieved and digitized at a sampling rate of \sim 1.0 Hz, and we finally selected their 10 horizontal

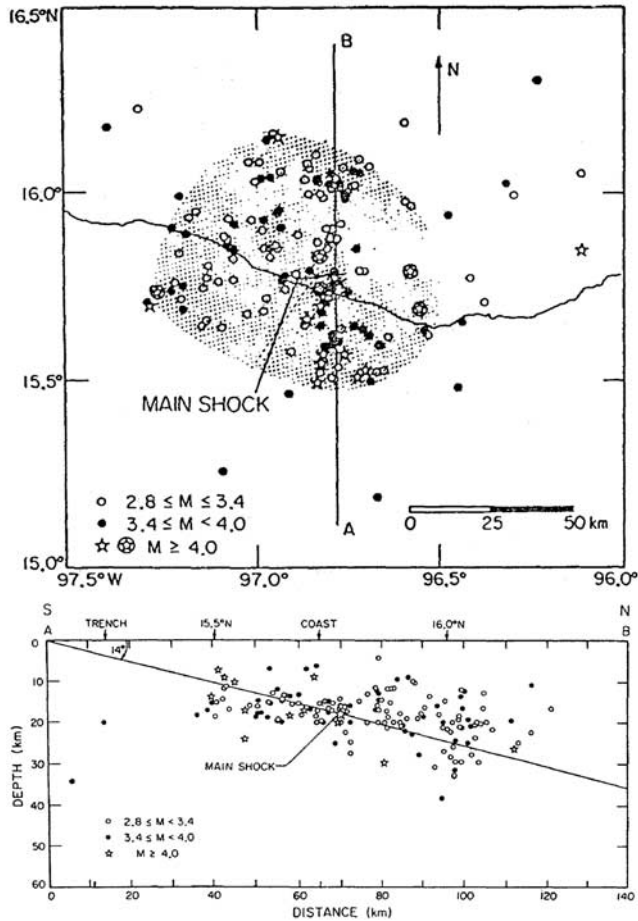


Figure 2. Aftershock distribution of the 29 November 1978 Oaxaca earthquake [Singh *et al.*, 1980]. (top) Horizontal projection, (bottom) vertical cross section along profile A-B. The fault plane dipping at 14° is from Stewart *et al.* [1981].

components from 10 stations located with a good azimuthal and distance coverage (see Figure 3d) for the present purpose. The kinematic waveform inversion essentially follows a linear inversion scheme formulated by Y. Yagi, which has been modified from Yoshida and Koketsu [1990]. The entire fault plane in the present case is divided into $9 \times 6 = 54$ subfaults, each having a size of 10 km \times 10 km. The Green's functions were calculated using the method of Kikuchi and Kanamori [1991], and the velocity structures used in this inversion are given in Tables 1a and 1b, where we refer to near-source regions and teleseismic receiver stations. The source time function at each subfault is expanded in seven overlapped triangles each with a duration of 2 s. The rupture front velocity is set at 3.2 km/s, which gives the start time of the basis function at each subfault. The inversion refers to the hypocenter determined from the local network. The slip vector on each subfault is represented by a linear combination of two orthogonal components. Figure 3a shows the fault plane solution, Figure 3b shows the moment rate function, and Figure 3c shows the total slip amplitudes with their slip vectors. The results show that large slip with a maximum exceeding 7 m is concentrated around the hypocenter located near the central part of the fault and that there are zones of medium slip around 1.5–2.0 m in the southeastern deeper fault and the northwestern shallower sections. The uncertainty in the estimated slip is $\sim 21\%$ of its maximum slip. Figure 3d compares the recorded and synthetic *P* waveforms at 10 stations, indicating a reasonable fit between them.

[8] On the other hand, the 30 September 1999 Oaxaca earthquake occurred in a location similar to that of the 1978 event (see Figure 1). The main shock was located at 16.00°N, 97.02°W at a focal depth of 40 km from local broadband seismograph observations [Singh *et al.*, 2000b]. The preliminary centroid moment tensor (CMT) solutions (Harvard, National Earthquake Information Center (NEIC), and Earthquake Research Institute (ERI), 2000) from teleseismic data provided slightly deviated epicentral locations with a centroid focal depth

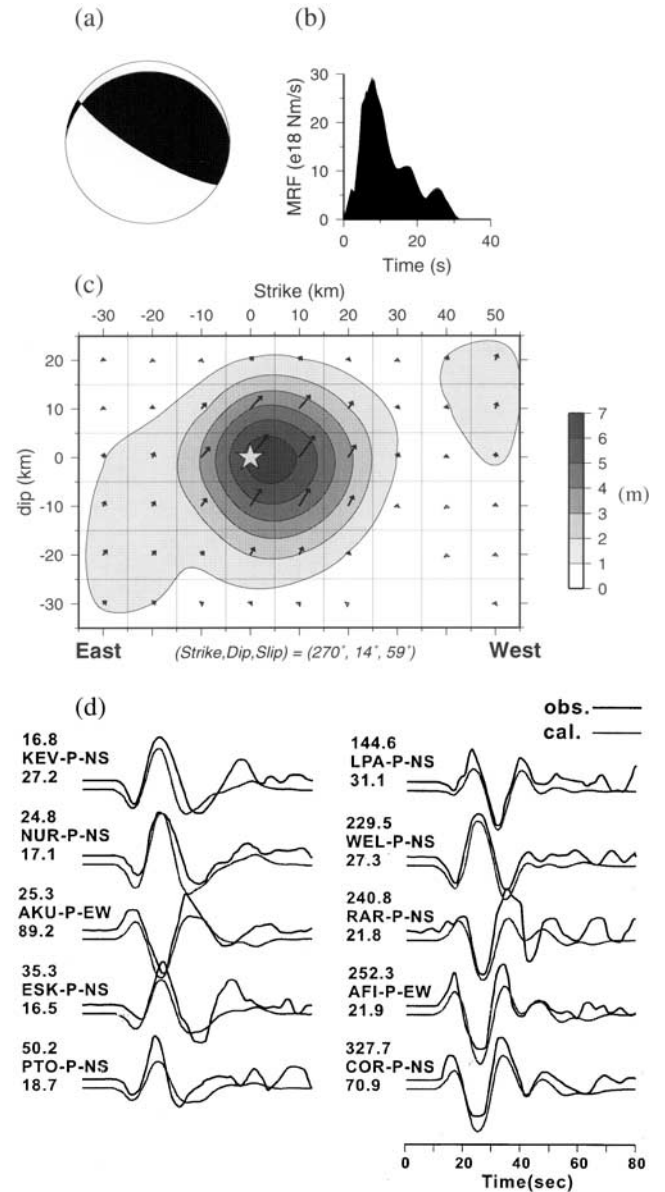


Figure 3. (a) Fault plane solution of the 1978 earthquake [after Stewart *et al.*, 1981], (b) the overall moment rate function, and (c) the coseismic slip distribution on the fault derived from waveform inversion. The maximum fault slip around the central part of the fault is 7.2 m. (d) Comparison between the WWSSN long-period records from the 1978 event (upper thick traces), and the corresponding synthetic waveforms calculated from the inversion (lower thin traces). The onset times are aligned at 10 s. The numbers above and below the station code indicate the station azimuth and the epicentral distance (in degrees), respectively.

Table 1a. Crust and Uppermost Mantle Structure Model Used in This Study for the Oaxaca Region, Mexico^a

Layer	H , km	V_p , km/s	V_s , km/s	ρ , g/cm ³	η , $\times 10^{19}$ Pa	τ , years
1	0	4.50	2.60	2.60		
2	1	5.30	3.06	2.70	10.0	100
3	5	6.20	3.58	2.75	5.0	100
4	15	6.85	3.95	2.90	5.0	40
5	30	8.15	4.71	3.20	2.5	5

^aFrom *Hernandez et al.* [2001]; modified after *Valdes et al.* [1986]. H , top depth to each layer; V_p , P wave velocity, V_s , S wave velocity; ρ density; η , Newtonian viscosity; τ , Maxwellian relaxation time. For the subducting slab, τ has been tentatively assumed to be 500 years. Layer 1 is used only to calculate Green's functions, but for dynamic calculations the thickness of layer 1 is included in layer 2.

ranging between 53 and 55 km, showing normal faulting mechanism with two nodal planes: $\delta = 51^\circ\text{--}55^\circ$, $\phi = 295^\circ\text{--}315^\circ$, slip of -81° to -83° and $\delta = 36^\circ\text{--}40^\circ$, $\phi = 103^\circ\text{--}120^\circ$, slip of -99° to -102° (Figure 1). The estimated seismic moment ranges between 1.3 and 2.0×10^{27} dyn cm. The slip distribution on the 1999 earthquake fault has been analyzed from inversion of seven local strong motion records [*Hernandez et al.*, 2001], together with 15 teleseismic P waveforms [*Yagi et al.*, 2001]. The two analyses, referring to the focal depth of 40 km determined from the local seismic network, give a smaller misfit between the recorded and synthetic waveforms for the nodal plane with a northeastward dip of 50° than for the other southwestward dipping nodal plane. This clearly indicates that the 1999 earthquake was a normal-faulting event with the fault dipping inland in the subducting Cocos plate. The solution by *Hernandez et al.* [2001] shows the main slip distributed at depths between 30 and 50 km with the highest slip of 2.5 m around 40–50 km over the fault located at depths from 25 to 55 km. On the other hand, *Yagi et al.* [2001] provided the fault extending from 34 km down to 62 km with the maximum slip of 2.3 m at depths around 47–52 km. More details of the latter results will be published in a future paper. The two solutions reveal large slip around the central part of the fault, although the pattern of slip distribution appears somewhat different.

[9] Figure 4 shows the side view of the 1978 thrust and the 1999 normal-faulting earthquakes with respect to the subducting slab. The fault widths of the two events are ~ 70 and ~ 40 km, respectively. It is clear that the 1999 earthquake occurred beneath the downdip edge of the 1978 thrust fault, although the relative location of the two events has a slight uncertainty both in the vertical and horizontal directions because of the somewhat less accurate hypocentral location of the 1978 event. We will now investigate if the occurrence of the 1999 normal-faulting event was actually affected by stress transfer from the 1978 thrust earthquake.

3. Coseismic Stress Change in the Subducting Plate

[10] In this section we estimate the coseismic stress change in and around the subducting plate due to the 1978 thrust earthquake on the basis of the slip distribution derived from the kinematic waveform inversion as observational constraints. For this purpose, we calculate coseismic change of all stress compo-

nents due to this earthquake, not only on its thrust fault plane but in the subducting plate, the overlying continental crust, and the uppermost mantle and in the asthenosphere. The model used here is an extension of a three-dimensional (3-D) dynamic model [*Mikumo and Miyatake*, 1993; *Mikumo et al.*, 1998, 1999], which incorporates a shallow dipping fault located on the upper interface of the subducting slab and embedded in a horizontally layered velocity structure. In this 3-D model we solve elastodynamic equations, incorporating the kinematic slip under appropriate boundary conditions with a second-order finite difference scheme. The boundary conditions imposed are (1) the continuity of the normal stress and normal displacement across the dipping fault, (2) the traction-free ground surface, (3) the continuity of all stress and displacement components at each of the layer interfaces, and (4) the absorbing boundary conditions [*Clayton and Engquist*, 1977] at the side and bottom of the model space. To evaluate the spatial distribution of dynamic and static stress changes, we calculate the distribution of fault slip for tentatively given static stress drop on the fault and then take the ratio between the already obtained kinematic slip and the calculated dynamic slip at each point on the fault. The ratio is multiplied by the previously assumed stress drop, and this iterative, least squares procedure is repeated until the RMS difference between the kinematic and dynamic slips over the fault can be minimized within a reasonably small value (say, 1% of the maximum slip). This gives a final model, for which we obtain not only the distribution of static stress drop on the fault but also the static stress change at all points in the specified 3-D model space.

[11] For numerical calculations we interpolated the kinematic slips previously obtained every 10 km into a grid size of 5 km and also extrapolated them to a fault size of 90 km \times 70 km. In stress calculations we used grid spacings of 5.0 km on the fault, 1.25 km in the vertical direction, and 4.85 km in the horizontal direction for a fault dip of 14.5° . The extent of the 3-D model space is taken as 400 km \times 105 km \times 340 km in the x , y , and z directions (see Figure 5), respectively, and the total time step is taken as 800 covering a time interval of 80 s. The layered velocity and density structure appropriate to the Oaxaca region is shown in Table 1a. Elastic wave velocities and densities in the subducting plate are tentatively assumed to be higher by 0, 5, and 10% than in the surrounding crust and mantle at the same depths.

[12] The spatial distribution of coseismic static stress change $\Delta\sigma_{y'z'}$ on the 1978 thrust fault is shown in Figure 6. The maximum stress drop near the center of the fault exceeds 220 bars (22 MPa), and the stress drop in the northwestern peripheral zones and in the southeastern deeper fault section (indicated by shaded zones) is <10 bars, while the stress increase in between these zones is >20 bars. We do not find any close correlation between the stress pattern and the spatial distribution of the 1978 aftershocks shown in Figure 2, but a few large aftershocks with magnitudes >4.0 may be seen in the outer zone of stress increase. Now, we look at static stress change in the subducting plate, in the vertical cross section A–A' marked in Figure 6. These stresses are resolved into two components $\Delta\sigma_{y'z'}$ (shear stress along the 1999 normal fault) and $\Delta\sigma_{z'z'}$ (tensional stress perpen-

Table 1b. Crust and Upper Mantle Structure Used for Teleseismic Receiver Stations^a

Layer	H , km	V_p , km/s	V_s , km/s	ρ , g/cm ³
1	0	5.57	3.36	2.65
2	15	6.50	3.74	2.87
3	33	8.10	4.68	3.30

^aFrom *Yagi et al.* [2001]. The parameters used here are the same as in Table 1a. For Green's functions the attenuation terms are included with $T/Q_p = 1.0$ s and $T/Q_s = 4.0$ s.

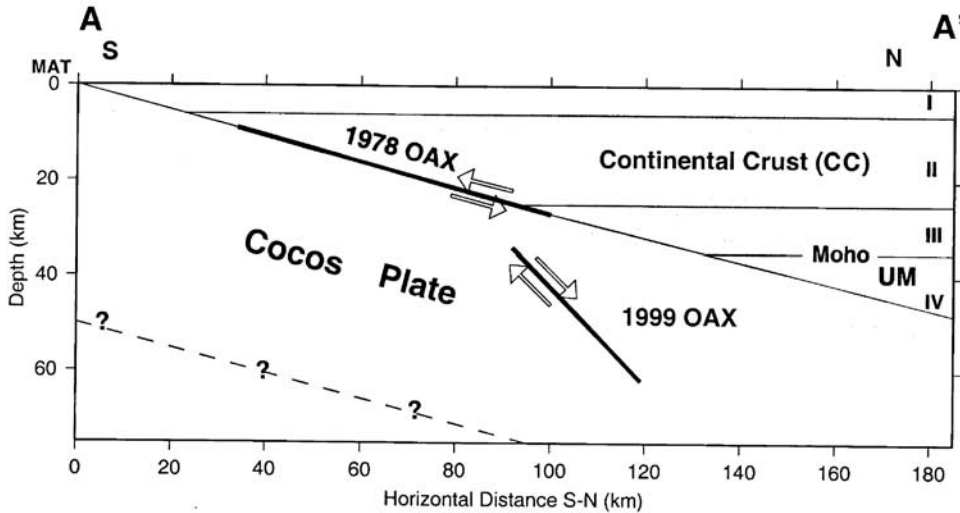


Figure 4. Side view of the 1978 thrust and the 1999 normal faults, with respect to the subducting Cocos plate. For the location of the 1978 fault, see *Stewart et al.* [1981], and for that of the 1999 fault see *Yagi et al.* [2001]. The relative location of the two events has a slight uncertainty because of the less accurate location of the 1978 event. The velocity and density structures in the overlying crust (CC) and the uppermost mantle (UM) are given in Table 1a.

dicular to this fault), where the y'' and z'' axes have been taken to be parallel and perpendicular to the 1999 fault. From the two components the Coulomb failure stress $\Delta\sigma_{cfs} = \Delta\sigma_{y''z''} + \mu' \Delta\sigma_{z''z''}$ is also calculated, where $\mu' = \mu(1 - p)$ is the apparent coefficient of friction for the effective pressure p [e.g., *King et al.*, 1994]. The most appropriate value of p is still not well known, but the effects of pore pressure p would reduce μ to $\sim 0.65-0.85$ estimated for solid friction [*Byerlee*, 1978]. For this reason, we tentatively take μ' in the range of 0.0 and 0.4, the latter of which has been assumed [*King et al.*, 1994] as an average. It has also been suggested [*Reasenber and Simpson*, 1992] that there is a best correlation between California seismicity rate and static stress change for the case of $\mu' = 0.1 \sim 0.3$, although these values are for the upper crust.

[13] Figure 7a shows the pattern of $\Delta\sigma_{y''z''}$, including three separate lobes of stress increase (indicated by open zones) above the updip portion and below the downdip portion and some far

beneath the thrust plane, while four lobes of stress decrease (indicated by shaded zones) extend continuously above and below the dipping fault. The 1999 fault zone is located in the zone of stress increase below the downdip edge of the 1978 thrust fault. On the other hand, the extensional stress change $\Delta\sigma_{z''z''}$ shows some increases above the updip and below the middle and downdip areas of the thrust plane, as shown in Figure 7b. Small patches of stress increase or decrease inside the zones with a reverse sign, and small bumps of the zero contours come from less accuracy around there in the course of the second-order finite difference calculations and interpolation procedures. The change in the Coulomb failure stress $\Delta\sigma_{cfs}$ for $\mu' = 0.4$ shown in Figure 7c indicates somewhat similar

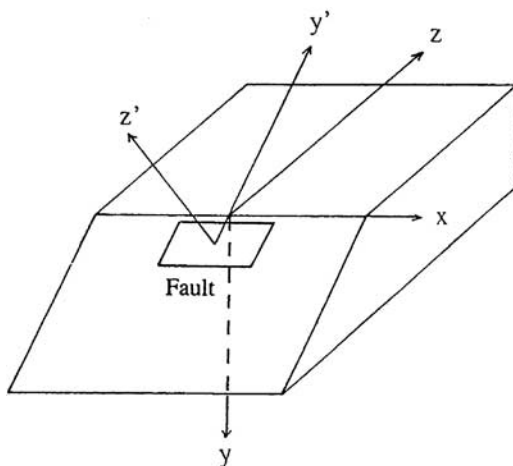


Figure 5. Location of a dipping thrust fault in a 3-D space, together with the coordinate axes used in this study. The x and y axes are taken parallel to the fault strike and downward vertically, and the y' and z' axes are taken parallel and perpendicular to the dipping fault, respectively.

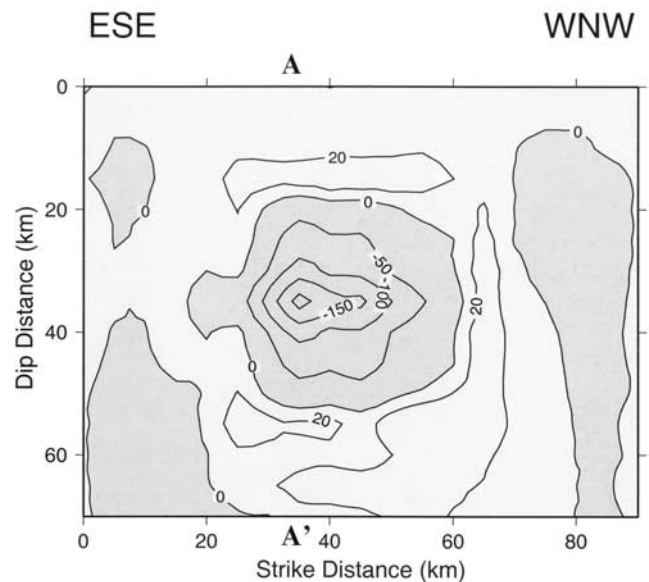
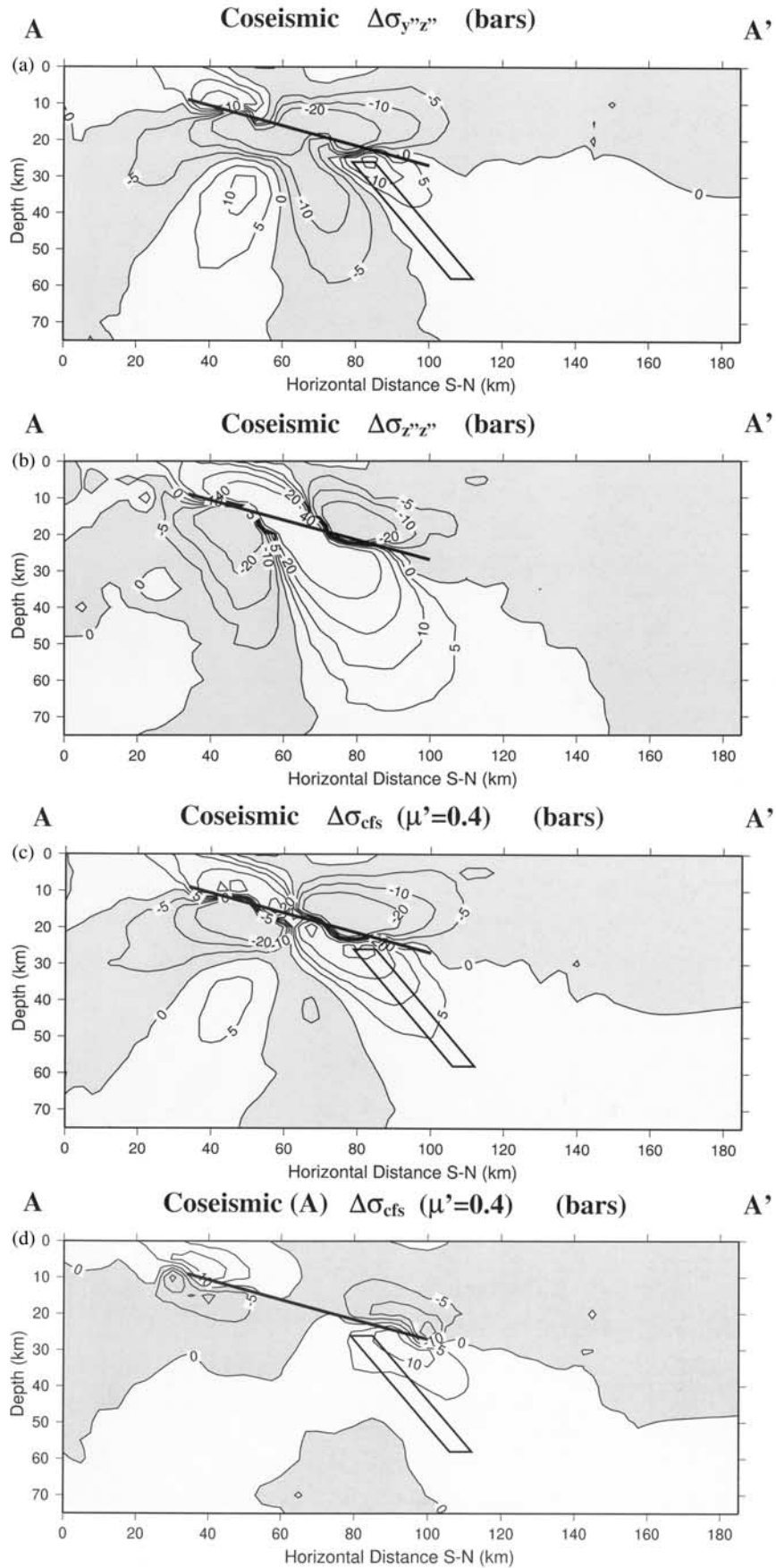


Figure 6. Coseismic stress change $\Delta\sigma_{y'z'}$ on the 1978 thrust fault. Shaded and open zones indicate the zones of stress decrease and increase, respectively, and the unit of stress on each contour is given in bars. Profile A-A' is taken across the portion of largest stress drop near the hypocenter.



but more pronounced patterns separated into three lobes of stress increase and decrease, respectively, than those of $\Delta\sigma_{y''z''}$, particularly below the middle and downdip portions of the 1978 thrust fault. It is clear that the 1999 normal-faulting earthquake took place in the zone of coseismic increase in the Coulomb failure stress and shear stress beneath the downdip edge of the 1978 dipping fault, even if the relative location between the two events has slight uncertainty as indicated by a narrow parallelogram for the latter event. The increase in the stresses in this zone reaches 5–15 bars (0.5–1.5 MPa), which is significantly large as compared with the increase reported so far [Harris, 1998]. This may be due to the proximity of the two events and partly to the heterogeneous stress change on the 1978 thrust fault. Although this amount varies slightly depending on the location and the width of the 1978 fault, their patterns are not affected very much. For comparison, the Coulomb failure stress change calculated from the simple slip distribution assumed with elliptical-shaped slip amplitudes is shown in Figure 7d. This gives a somewhat less pronounced pattern than that in Figure 7c, but the zones of stress increase and decrease are separated in a similar way, and the 1999 normal fault again falls into a wide zone of smaller stress increase. Accordingly, the 1978 thrust earthquake appears to have provided, at least, some effects to enhance the chance of the 1999 normal-faulting earthquake.

4. Postseismic Stress Change in the Subducting Plate

[14] Postseismic stress change in the subducting plate, which would affect the estimated coseismic change, may be caused by the following tectonic processes: (1) further (forward) aseismic slip on the ruptured fault segment or the updip or downdip extension of the thrust fault, (2) extensional stress due to the gravitational slab pull in the subduction process, (3) stress accumulation due to possible locking of the main thrust fault after interplate earthquakes, and (4) viscoelastic stress relaxation process in the overlying mantle and in the asthenosphere.

[15] Postseismic slip after large thrust events at subduction zones has been detected by geodetic data and recent GPS observations particularly around the Japanese Islands [e.g., Thatcher and Rundle, 1984a; Kawasaki et al., 1995; Heki et al., 1997; Hirose et al., 1999; Ito et al., 1999, 2000]. However, evidence of further aseismic slip on the 1978 thrust fault has not been obtained because of the lack of geodetic observations at that time, although it seems likely to have occurred. If it actually occurred on the major part of the fault with a few tens of percent of the coseismic slip, the postseismic increase of the shear stress beneath the thrust plane would enhance the coseismic stress change with this order of magnitude. If postseismic slip occurred on the updip extension of the fault, the coseismic stress increase beneath the downdip portion of the 1978 fault would be somewhat enhanced, but if it occurred on its downdip extension, the coseismic increase there would be slightly eroded. These possibilities remain unresolved. The slab pull due to the density contrast between the subducted slab and the surrounding mantle may not be large for such a shallow dipping slab as in the Mexican subduction zone, and also this may not be time-dependent. Steady state subduction at a uniform rate of plate convergence would not generate any stress change in the interior of the subducting plate except at the time of large interplate earthquakes. Accordingly, we will focus our attention to the last two

effects to estimate the postseismic changes of the coseismic effects, without taking into account the absolute tectonic loading stress.

4.1. Postseismic Stress Accumulation Due to Plate Convergence

[16] The steady state subduction at a constant rate of plate convergence gives a uniform slip over the upper boundary of the descending oceanic slab. The occurrence of interplate earthquakes is a perturbation of this steady state, providing an abrupt step-like slip on the main thrust zone. During the interseismic period this zone may be regarded as being locked if no after slip occurs, while the remaining part of the plate interface is still subjected to a uniform slip. The locking is represented by imposing a virtual backward (normal) slip at the plate convergence rate on the thrust zone [Savage, 1983]. The superposition of this back slip and a step slip would provide a solution to the surface deformation at subduction zones [Savage, 1983], as well as to internal stress accumulation in the subducting slab, during the interseismic period after interplate events. However, evidence is accumulated from recent geodetic measurements and GPS observations that the back slip to be considered is not uniform in space and time [Hashimoto and Jackson, 1993; Yoshioka et al., 1993; Ito et al., 1999, 2000; Sagiya, 1999; Dragert et al., 2001].

[17] Under the circumstance that no geodetic data are available, there could be two different concepts for the application of back slip. The first and more plausible approximation is that a spatially uniform back slip with a uniform rate of plate convergence should be imposed on the main thrust zone, while the second one is a spatially nonuniform back slip which could be a fraction of the nonuniform coseismic slip at each point on the fault.

[18] As a first step, we estimate stress accumulation in the subducting Cocos plate, with the first approximation, from a uniform back slip with a constant rate of plate convergence of 6 cm/yr (appropriate to the Oaxaca region) on the thrust fault plane. Following Matsu'ura and Sato [1989], the interseismic slip on the thrust fault, $D_p(x', y', t)$, may be written as

$$D_p(x', y', t) = -vtH(t) + D_c(x', y', T)H(t - T) \quad T < t < 2T, \quad (1)$$

where $D_c(x', y', T)$ is the coseismic slip at $t = T$ on the thrust fault plane ($x' - y'$), $vtH(t)$ is the steady state slip due to plate subduction, $-vtH(t)$ represents the virtual back slip, v is the plate convergence rate, and $H(t)$ is a unit impulse. Since the coseismic slip during the 1978 thrust earthquake has been found to be quite heterogeneous, D_c is a function of position on the two-dimensional fault, with large slip reaching 7 m near the center of the fault and medium slip in the surrounding zones, as shown in Figure 3a. In this case, D_p will remain positive in a limited zone of larger slip even after the recurrence time ($t > 2T$), while it drops to zero much earlier ($t < 2T$) in some part of the fault of smaller slip. Accordingly, we assume that the fault segments with a slip smaller than $6 \text{ cm/yr} \times 21 \text{ years}$ had been decoupled and started free slipping before the 1999 event, while the other segments with larger slip were still locked in 1999. In this sense, a part of the main thrust zone has been completely locked during the interseismic period. Under this assumption, we calculate postseismic stress change in the subducting slab for 21 years after the 1978 event, which corresponds to the time of the

Figure 7. (opposite) (a) Coseismic shear stress change $\Delta\sigma_{y''z''}$ along a vertical profile A–A' in the subducting plate. The y'' and z'' axes are taken parallel and perpendicular to the 1999 normal fault. Shaded and open zones indicate the zones of stress decrease and increase, respectively, with contours given in bars, and the bold line and slender parallelogram show the locations of the 1978 thrust fault and the possible range of the 1999 normal fault zone, respectively. The same explanations apply to Figures 7b–7d. (b) Coseismic extensional stress change $\Delta\sigma_{z''z''}$. (c) Coseismic change of the Coulomb failure stress $\Delta\sigma_{\text{cfs}} = \Delta\sigma_{y''z''} + \mu' \Delta\sigma_{z''z''}$ for the case of $\mu' = 0.4$. (d) Coseismic change of the Coulomb failure stress, which has been calculated from a simple, ellipsoidal slip distribution on the fault (see text).

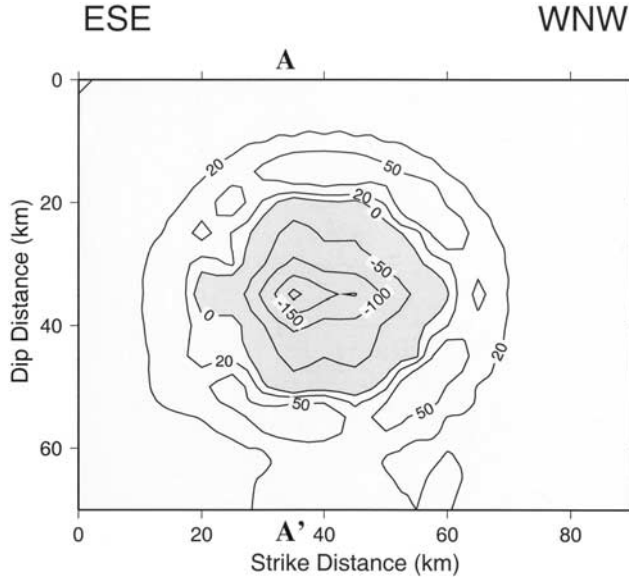


Figure 8. Postseismic stress state $\Delta\sigma_{yz}^{(p)}$ on the 1978 thrust fault 21 years after this event. Note that the zone of large stress drop around the central part of the fault shrinks and the zone of medium stress drop disappears. Compare with Figure 6.

1999 earthquake. Figure 8 shows the stress state $\Delta\sigma_{yz}^{(p)}$ in response to D_p on the 1978 thrust fault. Comparing this pattern with Figure 6a, we see that there still remains the zone of quite large stress drop around the center of the fault but that the zones of medium coseismic stress drop in the peripheral zones disappear.

[19] With the second concept, on the other hand, the rate of plate convergence on the thrust zone could be assumed proportional to $D_c(x', y', T)$. In this case, D_p would also be proportional to D_c and would decrease with time. Under this assumption the entire thrust zone will be completely locked during the recurrence period. The magnitude of the coseismic stress change will diminish according to the time elapsed, but the spatial pattern for the zones of stress increase and decrease will not be changed. All discussions on the coseismic stress change given in section 3 will be retained.

4.2. Viscoelastic Stress Relaxation

[20] To estimate the postseismic stress change, we incorporate viscoelastic stress relaxation process in the overlying lower crust, in the uppermost mantle, and in the asthenosphere. The stress-strain relation in a 3-D viscoelastic medium composed of a generalized Maxwell body may be written as [e.g., Mikumo, 1992]

$$\sigma_{kl} + \tau \dot{\sigma}_{kl} = \tau \left[\lambda \delta_{kl} \sum \dot{e}_{kk} + 2\mu \dot{e}_{kl} \right] \quad k, l = x, y, z, \quad (2)$$

where σ_{kl} and e_{kl} are the stress and strain tensors in the medium, λ and μ are Lamé's elastic constants, δ_{kl} is Kronecker's delta, and τ is the Maxwellian relaxation time given by

$$\tau = \exp(Q/RT_m) / 2\mu A \sigma_e^{n-1}. \quad (3)$$

Equation (3) has been derived from the experimental creep law [e.g., Kirby, 1980], $\dot{e} = A \sigma_e^n \exp(-Q/RT_m)$, where σ_e is the effective stress, T_m is the absolute temperature, R is the gas constant, and Q , A , and n are numerical constants. Since τ is the function of temperature and hence of the depth in the Earth, this may be written as $\tau(y)$. Although $\tau(y)$ would have to be estimated from (3), we simply give its rough estimate from $\tau(y) = \eta/\mu$, assigning the equivalent Newtonian viscosity η to the continental crust, the uppermost mantle, and the asthenosphere. Although there have been a variety of estimates of η covering a wide range, we tentatively assume the values given in Table 1a, which are taken from various sources [e.g.,

Freed and Lin, 1998, Figure 14], to estimate possible largest viscoelastic effects. Because the subducting slab may have essentially purely elastic properties, we tentatively assign $\tau = 500$ years to the slab, which is much longer than the recurrence time of large thrust earthquakes in this subduction zone.

[21] Equation (2) has two different types of solutions. One is the solution for the coseismic stress change $\Delta\sigma_{kl}^{(c)}(x, y, z, T)H(t)$ in response to $D_c(x', y', T)$, which is given by

$$\Delta\sigma_{kl}^{(1)}(x, y, z, t) = \Delta\sigma_{kl}^{(c)}(x, y, z, T) \exp[-(t-T)/\tau(y)]. \quad (4)$$

Equation (4) indicates the viscoelastic responses to $\Delta\sigma_{kl}^{(c)}$ that have been obtained in section 3, which are either negative or positive. Figure 9 shows temporal variations of $\Delta\sigma_{cfs}^{(1)}(x, y, z, t)$, indicating the viscoelastic relaxation of the calculated coseismic stress change $\Delta\sigma_{cfs}^{(c)}(x, y, z, T)$ at six selected points in the subducting slab (Figure 7c) up to 50 years after the 1978 earthquake. It can be seen that these variations are <10% during a postseismic period of 21 years.

[22] The other solution for long-term stress evolution $\Delta\sigma_{kl}^{(b)}(x, y, z, t)$ in response to the virtual back slip $-vH(t)$ may be given as

$$\begin{aligned} \Delta\sigma_{kl}^{(2)}(x, y, z, t) &= \tau(y) \left[\lambda \delta_{kl} \sum \dot{e}_{kk} + 2\mu \dot{e}_{kl} \right] \{1 - \exp[-(t-T)/\tau(y)]\} \\ &= -\tau(y) \Delta\sigma_{kl}^{(b)}(x, y, z, t) / (t-T) \{1 - \exp[-(t-T)/\tau(y)]\}. \end{aligned} \quad (5)$$

We calculate $-\Delta\sigma_{kl}^{(b)}(x, y, z, t)$ at $t-T=21$ years at each point in the 3-D space and then obtain the average rate of stress change $-\Delta\sigma_{kl}^{(b)}/(t-T)$ over the period. The total postseismic stresses $\Delta\sigma_{kl}^{(p)}$ are then obtained by

$$[\Delta\sigma_{kl}^{(p)} = \Delta\sigma_{kl}^{(1)} + \Delta\sigma_{kl}^{(2)}] \quad (6)$$

The results are shown below. For comparison, we made test calculations to estimate the approximate value of $\Delta\sigma_{kl}^{(p)}$ directly from $\Delta\sigma_{yz}^{(p)}$ given in Figure 8, without including the viscoelastic relaxation effects. Since the viscoelastic effects for 21 years are not very large, as shown in Figure 9, it was found that the present results obtained from (6), particularly their spatial patterns, are almost the same as those calculated approximately in the above way, although their absolute amplitudes are slightly different.

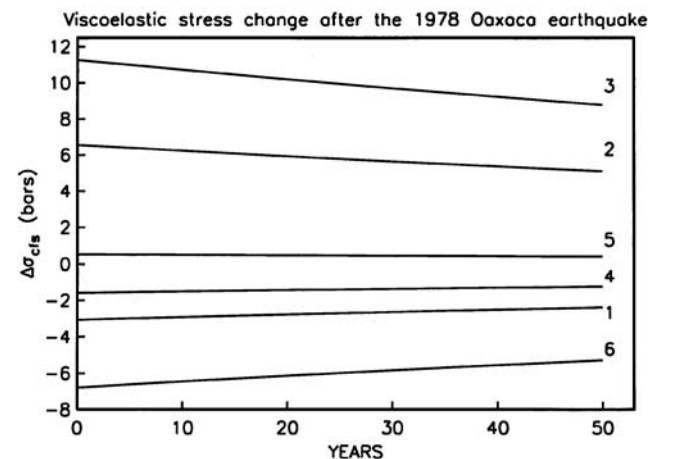


Figure 9. Viscoelastic relaxation of the Coulomb failure stress $\Delta\sigma_{cfs}^{(1)}$ (in bars) during 50 years at several selected points in the subducting plate. These locations are at 1 (114, 16), 2 (101, 36), 3 (90, 36), 4 (67, 66), 5 (52, 66), and 6 (33, 28), where the first and second numerals indicate the horizontal location measured from the left end in Figure 7c and the depth, each given in km.

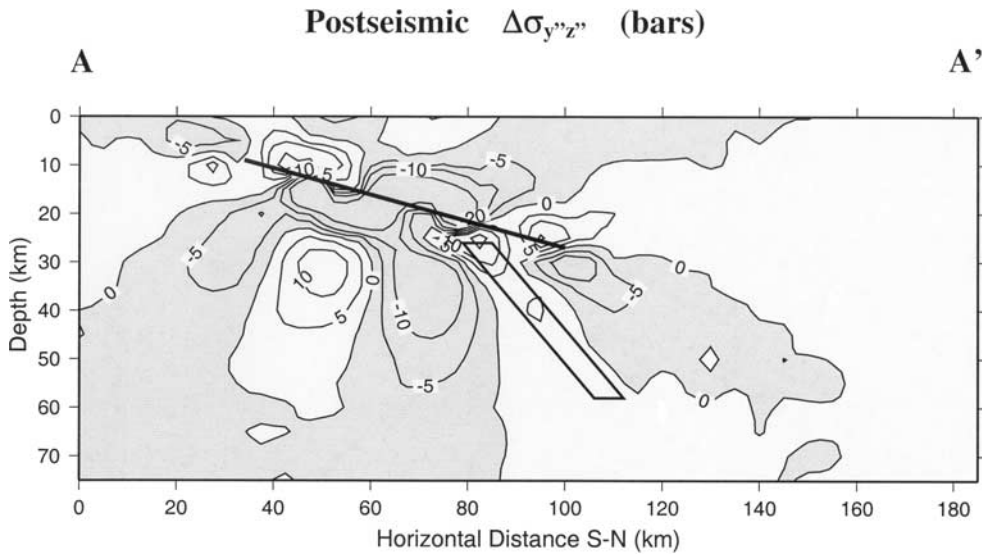


Figure 10a. Postseismic stress state $\Delta\sigma_{y'z'}^{(p)}$ at 21 years after the 1978 event along profile A–A' in the subducting plate. Note that the zones of stress decrease appear in the updip and downdip of the 1978 thrust fault. This comes from the locking of the large slip zone on the fault due to a back slip, and a free slip on the outer fault zone due to plate convergence. Compare with Figure 7a.

[23] The postseismic stress change $\Delta\sigma_{y'z'}^{(p)}$ 21 years after the 1978 event, including the two effects of stress accumulation due to plate convergence and viscoelastic relaxation, is shown in Figure 10a. We see that the stress pattern has changed to some extent from that of the coseismic change (Figure 7c). What is different is that the zones of stress decrease appear in the updip and downdip portions of the 1978 thrust fault, and hence the white zone of stress increase beneath the downdip edge shrinks. This is due to the locking of the large slip zone and the free slip on the surrounding fault zone. Even in this case, however, the 1999 normal fault zone is still located in the zone of stress increase. Figure 10b shows the corresponding postseismic change $\Delta\sigma_{cfs}^{(p)}$ of the Coulomb failure stress, which gives more complicated stress patterns. The zone of stress decrease expands further to the far-downdip portion of the thrust fault, while the zone of stress increase beneath the fault is more invaded. The location of the 1999 fault zone appears marginal

between the zones of stress increase and decrease, but there still remains the possibility that it might be included in the white zone because its relative location with respect to the 1978 fault has slight uncertainty. If we assume a slightly lower value of the apparent coefficient of friction, for example, $\mu' = 0.1-0.3$, which has been suggested by *Reasenber and Simpson* [1992], or $\mu' = 0.3$, which may give the optimal failure plane, as discussed in section 5, the stress pattern becomes closer to that of Figure 10a for $\mu' = 0$. In this case, the 1999 fault zone is clearly located in the zone of stress increase, as shown in Figure 10a. It is to be noted that similar calculations for 50 years after the thrust event (not shown here) give wider zones of stress decrease covering the 1999 fault zone, suggesting that normal-faulting events would not take place there 50 years later. Figure 11 shows the postseismic stress change $\Delta\sigma_{cfs}^{(p)}$ on the inferred 1999 normal fault, indicating that a quite large stress increase up to 15 bars remains in the upper part of the fault,

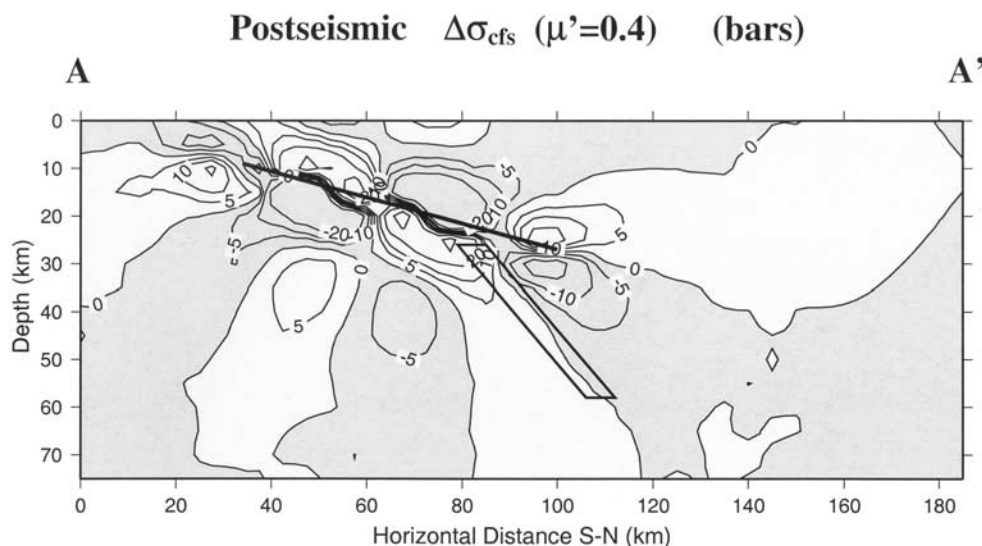


Figure 10b. Postseismic stress state $\Delta\sigma_{cfs}^{(p)}$ at 21 years after the 1978 event along profile A–A' in the subducting plate. Compare with Figure 7c.

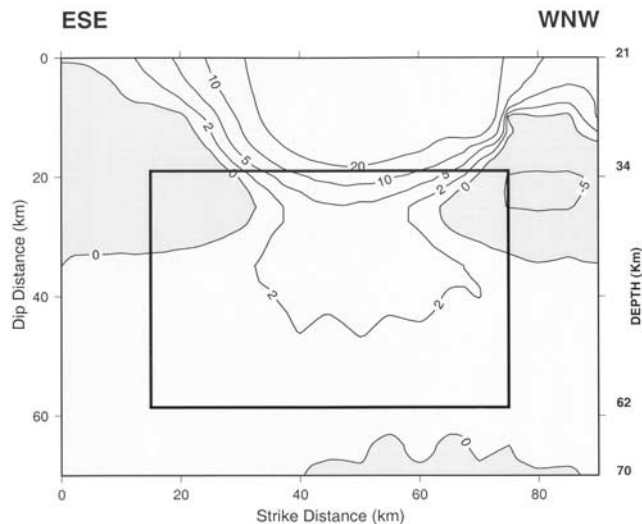


Figure 11. Postseismic stress change $\Delta\sigma_{\text{vis}}^{(p)}$ (for $\mu' = 0.3$) after the 1978 event on the dipping plane including the 1999 normal fault (enclosed by a bold square). Note that most parts of the fault had stress increase between 2 and 5 bars due to the 1978 thrust earthquake, while a large stress increase up to ~ 15 bars is observed near the upper part of the fault.

while the rest of the fault receives an increase of 2–5 bars. It is to be noted that five aftershocks of the 1999 earthquake, with magnitudes between 4.0 and 4.6, which are shown in Figure 1, take place at depths between 32 and 38 km [Singh *et al.*, 2000b]. As shown in Figure 10c and Figure 11, the slab at these depths still retained stress increase in 1999 due to the 1978 event, while this portion suffered either medium stress drop or small increase during the 1999 normal-faulting event [Yagi *et al.*, 2001]. It is possible that the combined effects of the stress change may have caused these large aftershocks with nearly the same mechanism as that of the 1999 main shock.

[24] All the above calculations strongly suggest that the effects of coseismic stress change due to the 1978 thrust earthquake are large enough not to vanish even 21 years after the event and hence that these effects could enhance the chance of occurrence of the 1999 normal-faulting earthquake.

5. Discussion

[25] We have estimated postseismic stress variations of the coseismic stress change in the subducting plate following a large thrust event. Temporal stress variations during a thrust earthquake cycle in and near a strongly coupled subducted slab has been discussed on the basis of 1-D dislocation and 2-D finite element modeling [e.g., Thatcher and Rundle, 1984b; Dmowska *et al.*, 1988; Taylor *et al.*, 1996], with a uniform seismic slip and a long-term rate of plate convergence including the viscoelastic relaxation process of the upper mantle. The latter two results show that the coseismic change in the uniaxial stress component below the thrust zone, either compressional or extensional, slowly recovers with time but still does not change its sign within the first half of the recurrence period. Dmowska *et al.* [1996] and Taylor *et al.* [1998] introduced 3-D finite element modeling to investigate the effects of asperities during the main subduction events on stress and deformation and their time variations not only in the slab but also in the overlying continental plate in relation to heterogeneous coupling along thrust interfaces. These are closely related to our work here, although they were interested mainly in the upper plate stressing and seismicity. Also, Gardi *et al.* [2000] introduced a 2-D finite element technique to model the stress field in a vertical cross

section of the subducting Cocos plate with different geometries, incorporating a plate convergence velocity and the slab pull and ridge push as the acting mechanism. In their models the main thrust zone is completely locked during the interseismic period after a thrust event with a uniform seismic slip. Their modeling results suggest that normal-faulting events could occur some time after the large thrust event in a wide zone of extensional stress below the downdip edge of the main thrust zone, in the form of flexural response of the overriding and subducting plates particularly to the specific, unbending, and subhorizontal geometry. Although their results seem sensitive to the geometry of the subducting slab, these could be an alternative explanation to the occurrence of intraplate normal-faulting earthquakes beneath a thrust fault event, particularly in the regions where the subducting plate actually has this type of geometry. In this case, the two effects from the coseismic and postseismic stress changes estimated from our calculations and from the flexural response to the plate geometry would be complementary to the cause of normal faulting earthquakes in the subducting Cocos plate. In the Oaxaca region, however, presently available seismicity data do not clearly indicate this type of specific geometry which is well documented for the Guerrero-Michoacan regions [e.g., Pardo and Suarez, 1995].

[26] Here we considered how and why the coseismic and postseismic stress increase due to the 1978 thrust event could enhance the chance of the 1999 normal-faulting earthquake, assuming that the latter event may have actually been activated 21 years after the former earthquake. One conceivable mechanism would be time-delayed fracture of the 1999 fault zone materials under a near-constant applied stress after the 1978 event, which is similar to static fatigue of materials due to stress corrosion. Many brittle materials exhibit time-dependent fracture when subjected to a long-term static load, as has been demonstrated by early laboratory experiments. While the experiments, mostly for metallic and nonmetallic materials including glass, ceramics, etc., have shown that the breaking strength is a logarithmic function of the time to failure [e.g., Anderson and Grew, 1977], a similar relation indicating static fatigue has been found in quartz and granite [Scholz, 1972]. Scholz [1968] has suggested that static fatigue phenomena due to stress corrosion could be the mechanism of creep in brittle rocks on a geological scale and also that time-dependent phenomena associated with earthquakes, such as aftershocks, multiple shocks, and delayed triggering of earthquakes by other earthquakes, might be explained by static fatigue. Since Scholz's [1972] experiments covering the time range up to 5×10^5 s indicate that the time delay is not solely dependent on the level of applied stress and its loading history but is also dependent on the environments such as temperature, ambient and pore pressures, and humidity, he proposed that the time-dependent transition probability of fracture $\mu(t)$ may be given in a form, $\mu(t) = 1/\{t\}$, where $\{t\}$ is the mean time to fracture. A similar form, $\mu(t) = \exp[-\beta\{\sigma(t) - S\}/k]$, has been proposed by Mogi [1962] and Scholz [1968], while Rundle and Jackson [1977] proposed a simpler form, $db(t)/dt = -\{\sigma(t) - S\}/\tau$, where $\sigma(t)$, $b(t)$, and S are the stress, breaking strength, and ultimate strength, respectively, and β , k , and τ are numerical constants. Thus $\{t\}$ may be related to the difference between $\sigma(t)$ and S . Although the above experiments were for small-scale rock specimens, the delay time would be extended to much longer time under natural conditions in the crust and the upper mantle. Unfortunately, however, there does not seem to be convincing experimental evidence covering the time range up to several tens of years.

[27] It is to be also noted that many rock materials existing in the lower crust and the uppermost mantle regions have a strong preferred orientation of their constituent minerals [Anderson and Grew, 1977] and hence that stress corrosion cracking would take place along this preferred orientation even under a similar stress state. If we take these relations and evidences into consideration, it seems possible that a large event could take place in the stressed

zone in different directions even 21 years after the previous event. However, since these experiments have been made under uniaxial stress conditions, their results might not be directly applicable to the present case involving a long-term increase of the shear and the Coulomb failure stresses. Under a constant normal stress with a slow increase of shear stress at remote distances, quasi-static shear failure will be nucleated in a small zone, depending on the roughness of preexisting weak planes and then will finally lead to dynamic rupture, as has been demonstrated by recent laboratory experiments [Ohnaka and Shen, 1999].

[28] Another problem is the orientation of the normal-faulting earthquakes that occurred beneath the thrust plane on the upper boundary of the subducting slab. While it has been shown in our previous study [Mikumo *et al.*, 1999; M. A. Santoyo *et al.*, manuscript in preparation, 2001] that the 1997 normal-faulting event took place with a nearly vertical fault plane beneath the ruptured fault zone of the 1985 earthquake, the 1999 normal-faulting event studied here had an oblique dip of $\sim 50^\circ$. The angles between these normal faults and the thrust faults of the preceding earthquakes are 76° and 36° , respectively. If both of these orientations exhibit the optimal orientation of the normal faults that have been created by the coseismic stress change due to the previous earthquakes, these should be a function of the effective coefficient of friction μ' and the regional stress field [King *et al.*, 1994]. Since the maximum regional compressive stress in the present two cases is more or less oriented parallel to the subducting direction of the downgoing slab and its magnitude may probably be around 10–30 MPa [e.g., Sekiguchi, 1985], the effects of the regional stress on the optimal direction would be less than several degrees and would not be much different for the two cases. In this case, the angles between the maximum compressive stress and the optimal failure plane, β , and μ' are related by $\cot 2\beta = \mu'$ [King *et al.*, 1994]. For the 1999 normal fault, μ' would be around 0.30 if we assume $\beta = 36^\circ$, but it is difficult to find an appropriate value of μ' for the 1997 normal fault under the above direction of the regional tectonic stress. Possible bending and unbending geometry of the plate subducting beneath the Michoacan region, which will give a slightly different direction of the maximum compressional stress, also does not provide a reasonable value of μ' .

[29] For these reasons, the fault orientations of the 1997 and 1999 normal faults would not necessarily be a manifestation of possible optimal orientations. Instead, the fault orientations might be different preferred orientations of preexisting weak planes originally involved in the oceanic lithosphere, which is now subducting. If so, we could speculate that the two normal-faulting events in the subducting plate might have resulted from reactivated preexisting weak planes by stress corrosion mechanism under coseismic stress increase due to the preceding large earthquakes and its long-term preservation during the postseismic period. However, further studies on this point are needed.

6. Conclusions

[30] Our stress estimates suggest that the coseismic stress increase due to the 1978 thrust earthquake may have enhanced the chance of occurrence of the 1999 normal-faulting earthquake in the subducting Cocos plate. The estimated maximum increase in the shear stress and the Coulomb failure stress below the downdip portion of the 1978 main thrust zone is ~ 0.5 – 1.5 MPa, which is significantly larger than those so far reported [e.g., Harris, 1998]. This may be due to the proximity of the two events and the large, heterogeneous stress drop during the thrust earthquake. The 1999 normal-faulting event took place in this zone of stress increase. Postseismic stress variations during 21 years resulting from the locking of the main thrust zone and also due to the viscoelastic stress relaxation change the coseismic stress patterns to some extent but are not large enough to overcome the effects of the coseismic change. If the coseismic and postseismic stress increase due to the

1978 earthquake actually triggered the 1999 event, one of the possible mechanisms might be static fatigue of fault zone materials due to stress corrosion. We speculate that the subducting oceanic lithosphere may have involved several, preexisting weak planes and one of these planes might have been reactivated and fractured due to stress corrosion under the applied stress there for 21 years.

[31] **Acknowledgments.** The senior author wishes to thank Jim Rice, Renata Dmowska, Shoichi Yoshioka, Manabu Hashimoto, and Takeshi Sagiya for their helpful discussions on many problems including the back slip at subduction zones. We are grateful to Ruth Harris (Associate Editor), Yehua Zeng, and an anonymous reviewer for their constructive comments on the manuscript. This work was stimulated by some discussions with Massimo Cocco, Annalisa Gardi, and others. We also thank Masayuki Kikuchi for a joint research program between Japanese and Mexican groups, which made this work possible, and Kazuko Noguchi for her cooperation in making the WWSSN records at Earthquake Research Institute, University of Tokyo, available to us. Our thanks are extended to Hiroo Kanamori, Eric Chael, and Michael Reichle for searching the WWSSN records and to Vladimir Kostoglodov for preparing one of the figures included. The present study is partially supported by the CONAcYt (Mexico) Project 32541-T, for which we thank the assistance of Raul Valenzuela.

References

- Abe, K., Lithospheric normal faulting beneath the Aleutian trench, *Phys. Earth Planet. Inter.*, 5, 90–98, 1972a.
- Abe, K., Mechanisms and tectonic implications of the 1966 and 1970 Peru earthquakes, *Phys. Earth Planet. Inter.*, 5, 367–379, 1972b.
- Abe, K., Tectonic implications of the large Shioya-oki earthquake of 1938, *Tectonophysics*, 41, 269–289, 1977.
- Anderson, O. L., and P. C. Grew, Stress corrosion theory of crack propagation with application to geophysics, *Rev. Geophys.*, 15, 77–105, 1977.
- Byerlee, J. D., Friction in rocks, *Pure Appl. Geophys.*, 116, 615–626, 1978.
- Chael, E. P., and G. S. Stewart, Recent large earthquakes along the Middle American trench and their implications for the subduction process, *J. Geophys. Res.*, 87, 329–338, 1982.
- Christensen, D. H., and T. Lay, Large earthquakes in the Tonga region associated with subduction of the Louisville ridge, *J. Geophys. Res.*, 93, 13,367–13,389, 1988.
- Clayton, R., and B. Engquist, Absorbing boundary conditions for acoustic and wave equations, *Bull. Seismol. Soc.*, 67, 1529–1540, 1977.
- Cocco, M., M. J. Pacheco, S. K. Singh, and F. Courboulex, The Zihuatanejo, Mexico, earthquake of 1994 December 10 ($M = 6.6$): Source characteristics and tectonic implications, *Geophys. J. Int.*, 131, 135–145, 1997.
- Dmowska, R., J. R. Rice, L. C. Lovinson, and D. Josell, Stress transfer and seismic phenomena in coupled subduction zones during the earthquake cycles, *J. Geophys. Res.*, 93, 7869–7884, 1988.
- Dmowska, R., G. Zheng, and J. R. Rice, Seismicity and deformation at convergence margins due to heterogeneous coupling, *J. Geophys. Res.*, 101, 3015–3029, 1996.
- Dragert, H., K. Wang, and T. S. James, A silent slip event on the deeper Cascadia subduction interface, *Science*, 292, 1525–1528, 2001.
- Eissler, H., and H. Kanamori, A large normal-fault earthquake at the junction of the Tonga trench and Louisville ridge, *Phys. Earth Planet. Inter.*, 29, 161–172, 1982.
- Freed, A. M., and J. Lin, Time-dependent changes in failure stress following thrust earthquakes, *J. Geophys. Res.*, 103, 24,393–24,409, 1998.
- Gardi, A., M. Cocco, A. M. Negro, R. Sabadini, and S. K. Singh, Dynamic modeling of the subduction zone of central Mexico, *Geophys. J. Int.*, 143, 809–820, 2000.
- Harris, R., Introduction to special section: Stress triggers, stress shadows, and implications for seismic hazards, *J. Geophys. Res.*, 103, 24,347–24,358, 1998.
- Hashimoto, M., and D. D. Jackson, Plate tectonics and crustal deformation around the Japanese Islands, *J. Geophys. Res.*, 98, 16,149–16,166, 1993.
- Heki, K., S. Miyazaki, and H. Tsuji, Silent fault slip following and interplate thrust earthquake at the Japan trench, *Nature*, 386, 595–598, 1997.
- Hernandez, B., N. M. Shapiro, S. K. Singh, J. F. Pacheco, F. Cotton, M. Campillo, A. Iglesias, V. Cruz, J. M. Gomez, and L. Alcantara, Rupture history of September 30, 1999 intraplate earthquake of Oaxaca, Mexico ($M_w = 7.5$) from inversion of strong-motion data, *Geophys. Res. Lett.*, 28, 363–366, 2001.
- Hirose, H., K. Hirahara, F. Kimata, N. Fujii, and S. Miyazaki, A slow thrust slip event following the two 1996 Hyuganada earthquakes beneath the Bungo channel, southwest Japan, *Geophys. Res. Lett.*, 26, 3237–3240, 1999.

- Ito, T., S. Yoshioka, and S. Miyazaki, Interplate coupling in southwest Japan deduced from inversion analysis of GPS data, *Phys. Earth Planet. Inter.*, 115, 17–34, 1999.
- Ito, T., S. Yoshioka, and S. Miyazaki, Interplate coupling in northeast Japan deduced from inversion analysis of GPS data, *Earth Planet Sci. Lett.*, 176, 117–130, 2000.
- Kanamori, H., Seismological evidence for a lithospheric normal faulting—The Sanriku earthquake of 1933, *Phys. Earth Planet. Inter.*, 4, 289–300, 1971.
- Kausel, E., and J. Campos, The $M_s = 8$ tensional earthquake of 9 December 1950 of northern Chile and its relation to the seismic potential of the region, *Phys. Earth Planet. Inter.*, 72, 220–235, 1992.
- Kawasaki, I., Y. Asai, Y. Tamura, T. Sagiya, N. Mikami, Y. Okada, M. Sakata, and M. Kasahara, The 1992 Sanriku-Oki, Japan, ultra-slow earthquake, *J. Phys. Earth*, 43, 105–116, 1995.
- Kikuchi, M., and H. Kanamori, Inversion of complex body waves, III, *Bull. Seismol. Soc. Am.*, 81, 2335–2350, 1991.
- King, G. C. P., R. S. Stein, and J. Lin, Static stress changes and the triggering of earthquakes, *Bull. Seismol. Soc. Am.*, 84, 935–953, 1994.
- Kirby, S. H., Tectonic stresses in the lithosphere: Constraints provided by experimental deformation of rocks, *J. Geophys. Res.*, 85, 6353–6363, 1980.
- Lundgren, P., and E. A. Okal, Slab decoupling in the Tonga arc: The June 22, 1977, earthquake, *J. Geophys. Res.*, 93, 13,355–13,366, 1988.
- Lynnes, C. S., and T. Lay, Source process of the great Sumba earthquake, *J. Geophys. Res.*, 93, 13,407–13,420, 1988.
- Masters, T. G., J. Berger, and F. Gilbert, Observations from the IDA network of the moment tensor of the Oaxaca earthquake, November 29, 1978, *Geofis. Int.*, 17, 281–286, 1980.
- Matsu'ura, M., and T. Sato, A dislocation model for the earthquake cycle at convergent plate boundaries, *Geophys. J. Int.*, 96, 23–32, 1989.
- McNally, K. C., and J. B. Minster, Nonuniform seismic slip rates along the Middle America trench, *J. Geophys. Res.*, 86, 4949–4959, 1981.
- Mendoza, C., and S. Hartzell, Slip distribution of the 19 September 1985 Michoacan, Mexico, earthquake: Near-source and teleseismic constraints, *Bull. Seismol. Soc. Am.*, 79, 655–669, 1989.
- Mikumo, T., Dynamic fault rupture and stress recovery processes in continental crust under depth-dependent shear strength and frictional parameters, *Tectonophysics*, 211, 201–222, 1992.
- Mikumo, T., and T. Miyatake, Dynamic rupture processes on a dipping fault, and estimates of stress drop and strength excess from the results of waveform inversion, *Geophys. J. Int.*, 112, 481–496, 1993.
- Mikumo, T., T. Miyatake, and M. A. Santoyo, Dynamic rupture of asperities and stress change during a sequence of large intraplate earthquakes in the Mexican subduction zone, *Bull. Seismol. Soc. Am.*, 88, 686–702, 1998.
- Mikumo, T., S. K. Singh, and M. A. Santoyo, A possible stress interaction between large thrust and normal faulting earthquakes in the Mexican subduction zone, *Bull. Seismol. Soc. Am.*, 89, 1418–1427, 1999.
- Mikumo, T., M. A. Santoyo, and S. K. Singh, Dynamic rupture and stress change in a normal faulting earthquake in the subducting Cocos plate, *Geophys. J. Int.*, 140, 611–620, 2000.
- Mogi, K., Study of elastic shocks caused by the fracture of heterogeneous materials and its relation to earthquake phenomena, *Bull. Earthquake Res. Inst. Univ. Tokyo*, 40, 125–173, 1962.
- Ohnaka, M., and L. F. Shen, Scaling of the shear rupture process from nucleation to dynamic propagation: Implications of geometric irregularity of the rupturing surfaces, *J. Geophys. Res.*, 104, 817–844, 1999.
- Pardo, M., and G. Suarez, Shape of the subducted Rivera and Cocos plates in southern Mexico: Seismic and tectonic implications, *J. Geophys. Res.*, 100, 12,357–12,373, 1995.
- Ponce, L., K. C. MacNally, V. Sumin de Pontilla, J. Gonzales, A. Castillo, L. Gonzales, E. P. Chael, and M. French, Oaxaca, Mexico earthquake of 29 November 1978: A preliminary report on spatio-temporal pattern of preceding seismic activity and mainshock relocation, *Geofis. Int.*, 17, 109–126, 1980.
- Reasenber, P. A., and R. W. Simpson, Response of regional seismicity to the static stress change produced by the Loma Prieta earthquake, *Science*, 255, 1687–1690, 1992.
- Reichle, M. S., K. Priestley, J. Brune, and J. A. Orcutt, The 1978 Oaxaca earthquake source mechanism analysis from digital data, *Geofis. Int.*, 17, 295–302, 1980.
- Rundle, J. B., and D. D. Jackson, Numerical simulation of earthquake sequence, *Bull. Seismol. Soc. Am.*, 67, 1363–1377, 1977.
- Sagiya, T., Interplate coupling in the Tokai district, central Japan, deduced from continuous GPS data, *Geophys. Res. Lett.*, 26, 2315–2318, 1999.
- Savage, J. C., A dislocation model of strain accumulation and release at a subduction zone, *J. Geophys. Res.*, 88, 4984–4996, 1983.
- Scholz, C. H., Microfractures, aftershocks, and seismicity, *Bull. Seismol. Soc. Am.*, 58, 1117–1130, 1968.
- Scholz, C. H., Static fatigue of quartz, *J. Geophys. Res.*, 77, 2104–2114, 1972.
- Sekiguchi, S., The magnitude of driving forces of plate motion, *J. Phys. Earth*, 33, 369–389, 1985.
- Singh, S. K., J. Havskov, K. MacNally, L. Ponce, T. Hearn, and M. Vassiliou, The Oaxaca, Mexico, earthquake of 19 November 1978: A preliminary report of aftershocks, *Science*, 207, 1211–1213, 1980.
- Singh, S. K., L. Astiz, and J. Havskov, Seismic gaps and recurrence periods of large earthquakes along the Mexican subduction zone: A re-examination, *Bull. Seismol. Soc. Am.*, 71, 827–843, 1981.
- Singh, S. K., G. Suarez, and T. Dominguez, The Oaxaca, Mexico earthquake of 1931: Lithospheric normal faulting in the subducted Cocos plate, *Nature*, 317, 56–58, 1985.
- Singh, S. K., J. Pacheco, T. Mikumo, and V. Kostoglodov, Intraplate earthquakes in central Mexico and their relationship with large/great interplate thrust earthquakes, paper presented at the Annual Meeting, Seismol. Soc. of Am., San Diego, Calif., 2000a.
- Singh, S. K., et al., The Oaxaca earthquake of 30 September 1999 ($M_w = 7.5$): A normal-faulting event in the subducted Cocos plate, *Seismol. Res. Lett.*, 71, 67–78, 2000b.
- Spence, W., The 1977 Sumba earthquake series: Evidence for slab pull force acting at a subduction zone, *J. Geophys. Res.*, 91, 7225–7239, 1986.
- Stewart, G. S., E. P. Eric, and K. C. McNally, The November 29, 1978, Oaxaca, Mexico, earthquake: A large simple event, *J. Geophys. Res.*, 86, 5053–5060, 1981.
- Taylor, M. A. J., G. Zheng, J. R. Rice, W. D. Stuart, and R. Dmowska, Cyclic stressing and seismicity at strongly coupled subduction zones, *J. Geophys. Res.*, 101, 8361–8381, 1996.
- Taylor, M. A. J., R. Dmowska, and J. R. Rice, Upper plate stressing and seismicity in the subduction earthquake cycle, *J. Geophys. Res.*, 103, 24,521–24,542, 1998.
- Thatcher, W., and J. B. Rundle, The earthquake deformation cycle and the Nankai trough, southwest Japan, *J. Geophys. Res.*, 89, 3087–3101, 1984a.
- Thatcher, W., and J. B. Rundle, A viscoelastic coupling model for the cyclic deformation due to periodically repeated earthquakes at subduction zones, *J. Geophys. Res.*, 89, 7632–7640, 1984b.
- Valdes, C., W. D. Mooney, S. K. Singh, R. P. Meyer, C. Lomnitz, J. H. Lueterget, C. E. Helsley, B. T. R. Lewis, and M. Mena, Crustal structure of Oaxaca, Mexico from seismic refraction measurements, *Bull. Seismol. Soc. Am.*, 76, 547–563, 1986.
- Ward, S. N., A technique for the recovery of the seismic moment tensor applied to the Oaxaca, Mexico earthquake of November 1978, *Bull. Seismol. Soc. Am.*, 70, 717–734, 1980.
- Yagi, Y., M. Kikuchi, and T. Mikumo, Source process of the Sept. 30, 1999 Oaxaca, Mexico earthquake, and its relationship to the stress change due to a past earthquake, paper presented at the Joint Meeting of the Earth and Planetary Sciences of Japan, Toyko, 2001.
- Yoshida, S., and K. Koketsu, Simultaneous inversion of waveform and geodetic data for the rupture process of the 1984 Nagano-ken-seibu, Japan, earthquake, *Geophys. J. Int.*, 103, 355–362, 1990.
- Yoshida, Y., K. Satake, and K. Abe, The large normal faulting Mariana earthquake of April 5, 1990 in coupled subduction zone, *Geophys. Res. Lett.*, 19, 297–300, 1992.
- Yoshioka, S., T. Yabuki, T. Sagiya, T. Tada, and M. Matsu'ura, Interplate coupling and relative plate motion in the Tokai district, central Japan, deduced from geodetic data inversion using ABIC, *Geophys. J. Int.*, 113, 607–621, 1993.

T. Mikumo, M. A. Santoyo, and S. K. Singh, Instituto de Geofisica, Universidad Nacional Autonoma de Mexico, Del Coyoacan, Mexico 04510 D.F., Mexico. (mikumo@ollin.igeofcu.unam.mx; mas@ollin.igeofcu.unam.mx; krishna@ollin.igeofcu.unam.mx)

Y. Yagi, Earthquake Research Institute, University of Tokyo, Yayoi 1-1-1, Bunkyo, Tokyo 113-0032, Japan. (yuji@eri.u-tokyo.ac.jp)